Yi Lin and Zhongjie Sun

# In Vivo Pancreatic β-Cell–Specific Expression of Antiaging Gene *Klotho*: A Novel Approach for Preserving β-Cells in Type 2 Diabetes

*Diabetes 2015;64:1444–1458 | DOI: 10.2337/db14-0632*

PHARMACOLOGY AND THERAPEUTICS

**Protein expression of an antiaging gene, *Klotho*, was depleted in pancreatic islets in patients with type 2 diabetes mellitus (T2DM) and in *db*/*db* mice, an animal model of T2DM. The objective of this study was to investigate whether in vivo expression of Klotho would preserve pancreatic β-cell function in *db*/*db* mice. We report for the first time that β-cell–specific expression of Klotho attenuated the development of diabetes in *db*/*db* mice. β-Cell–specific expression of Klotho decreased hyperglycemia and enhanced glucose tolerance. The beneficial effects of Klotho were associated with significant improvements in T2DM-induced decreases in number of β-cells, insulin storage levels in pancreatic islets, and glucose-stimulated insulin secretion from pancreatic islets, which led to increased blood insulin levels in diabetic mice. In addition, β-cell–specific expression of Klotho decreased intracellular superoxide levels, oxidative damage, apoptosis, and DNAJC3 (a marker for endoplasmic reticulum stress) in pancreatic islets. Furthermore, β-cell–specific expression of Klotho increased expression levels of Pdx-1 (insulin transcription factor), PCNA (a marker of cell proliferation), and LC3 (a marker of autophagy) in pancreatic islets in *db*/*db* mice. These results reveal that β-cell–specific expression of Klotho improves β-cell function and attenuates the development of T2DM. Therefore, in vivo expression of Klotho may offer a novel strategy for protecting β-cells in T2DM.**

Diabetes affects ~150 million people worldwide, and this figure is expected to double in the next 20 years (1). About 90–95% of all North American cases of diabetes are type 2 diabetes mellitus (T2DM) (1). Physiologically, pancreatic β-cells constantly synthesize insulin, which is stored within vacuoles and released once triggered by an elevation in blood glucose level. Insulin is the principal hormone that regulates uptake of glucose from the blood into most cells, including skeletal muscle cells and adipocytes. Insulin also is the major signal that promotes the conversion of glucose to glycogen for internal storage in liver and skeletal muscle cells. For many years, T2DM was recognized only owing to insulin resistance, but now, there exists a common agreement that T2DM is a complex pathophysiologic spectrum that includes insulin resistance and β-cell failure. Significant β-cell failure is now believed to take place at an early stage in disease progression; that is, β-cell function declines sharply before and after the diagnosis of T2DM (2). In the UK Prospective Diabetes Study, for example, the secretory capacity of β-cells was reduced by 50% at the time fasting hyperglycemia was diagnosed (3). Generally, the compensatory ability of the β-cell with respect to an increase in insulin resistance keeps blood glucose at the near-normal level through proportionate enhancements of β-cell function (4). No hyperglycemia exists without β-cell dysfunction (5). Maintaining recommended targets of blood glucose control is difficult for many patients with T2DM because of the progressive loss of β-cell function; thus, one of the goals in the treatment of T2DM is to preserve functional β-cells in pancreatic islets.

Department of Physiology, College of Medicine, University of Oklahoma Health Sciences Center, Oklahoma City, OK

Corresponding author: Zhongjie Sun, zhongjie-sun@ouhsc.edu.

Received 21 April 2014 and accepted 31 October 2014.

This article contains Supplementary Data online at http://diabetes.diabetesjournals.org/lookup/suppl/doi:10.2337/db14-0632/-/DC1.

The mouse *Klotho* (also called *α Klotho*) gene contains five exons and encodes a single-pass transmembrane protein with 1,014 amino acids predominantly expressed in the kidney and the brain choroid plexus (6). The majority of amino acids in the Klotho peptide resides in the amino-terminal extracellular domain, which is followed by a 21-amino acid transmembrane domain and an 11-amino acid short intracellular carboxyl terminus (6). Two forms of Klotho exist—the full-length Klotho (130 kDa) and the short-form Klotho (65 kDa)—that can be generated by alternative RNA splicing or proteolytic cleavage (6,7). Overexpression of Klotho extends life span in mice, whereas mutation of the *Klotho* gene causes multiple premature aging phenotypes and shortened life span (6,8). Klotho has been reported to function as a cofactor for activation of fibroblast growth factor (FGF) receptor 1c by FGF23 in the regulation of calcium, phosphate, and vitamin D metabolism in the kidneys (9). *Klotho*$^{-/-}$ mutant mice exhibit pancreatic islet atrophy, decreases in insulin content and mRNA levels in pancreatic islets, and decreases in serum insulin levels (10). Most recently, we reported that *Klotho* mRNA and proteins are expressed in mouse pancreatic islets and that silencing of Klotho impaired glucose-stimulated insulin secretion in MIN6 β-cells (11). However, whether Klotho expression is altered in pancreatic β-cells in T2DM is not known and whether it protects β-cell function in T2DM has never been investigated.

The *db/db* mouse was originally derived from an autosomal recessive mutation in the db gene, which encodes for leptin receptors. This model resembles key features of human T2DM, including peripheral insulin resistance and progressive deterioration of pancreatic β-cells (12). Our preliminary study showed that the Klotho level in pancreatic islets is decreased significantly in patients with T2DM and in *db/db* mice, an animal model of T2DM. The objective of the current study was to investigate whether β-cell–specific expression of Klotho protects β-cell function and attenuates the development of diabetes in *db/db* mice.

## RESEARCH DESIGN AND METHODS

### Cell Culture

Pancreatic insulinoma MIN6 β-cells were provided by J. Miyazaki (School of Medicine, Kumamoto University, Kumamoto, Japan) and D.F. Steiner (University of Chicago, Chicago, IL) (13). MIN6 cells were cultured and maintained in DMEM containing 25 mmol/L glucose, 10% FBS, 1% penicillin/streptomycin, 2 mmol/L glutamine, and 100 μmol/L β-mercaptoethanol. MIN6 β-cells of <20 passages were used in this experiment. The 3T3-L1 preadipocytes and mouse renal inner medullary collecting duct (mIMCD3) cells were cultured in these media without β-mercaptoethanol.

### Human Pancreas

The use of human pancreas was approved by the Institutional Review Board at the University of Oklahoma Health Sciences Center. Human pancreata from normal donors (age 37–50, both sexes) and T2DM donors (age 42–49, both sexes) were obtained from the National Disease Research Interchange, National Resource Center (Philadelphia, PA).

### Adeno-Associated Virus Vector Construction and Recombinant Viral Production

The procedures for plasmid construction and adeno-associated virus (AAV) packaging were described in our previous studies (14,15). Plasmid of pAAV2.1-mINSULIN-nLacZ with 1.13-Kb mouse *preproinsulin gene II* promoter was provided by X. Xiao (Eshelman School of Pharmacy, University of North Carolina at Chapel Hill, Chapel Hill, NC) (16). A plasmid of pEFmKLcFT with the full-length mouse *Klotho* cDNA and COOH-terminal FLAG-tag was provided by M. Kuro-O (The University of Texas Southwestern Medical Center, Dallas, TX). The full-length *Klotho* cDNA with the COOH-terminal Flag-tag (3.1 kb in total) was cloned into AAV serotype 2 (AAV2) (Stratagene, La Jolla, CA). The mouse *insulin II* promoter was cloned into AAV2 by replacing the original *CMV* promoter and intron. The *insulin II* promoter and *GFP* cDNA (700 base pairs [bp]) were cloned into the AAV2 vector as the control constructs. The constructs of pAAV-mKL and pAAV-GFP were then packaged with pHelper and pAAV-RC to produce recombinant AAVs by following the manufacturer's instruction manual (Stratagene). Recombinant viruses were purified through a CsCl gradient as previously described (17). The titers of recombinant viral genome particles were determined on a Bio-Rad CFX96 Real-Time PCR Detection System with a pair of primers targeted to the *insulin II* promoter region (forward [F]: 5′-AAATGCTCAGCCAAGGACAA-3′; reverse [R]: 5′-GGAC TTTGCTGTTTGACCCATT-3′) and with the method previously described (18,19). For the remainder of this article, these recombinant viruses will be referred as rAAV-GFP and rAAV-mKL, respectively.

### Transfection With Plasmid DNA

Plasmid DNA, including pAAV-mKL, pAAV-GFP, and pAAV-CMV-mKL, were purified with the QIAGEN Plasmid Maxi Kit. MIN6 cells, 3T3-L1 preadipocytes, and mIMCD3 cells cultured in a six-well plate were transfected with various plasmid DNAs at a concentration of 0.072 μg/mL using Optifect reagent according to the manufacturer's protocol followed by 48-h incubation in DMEM with 10% FBS at 37°C in a 5% $CO_2$ incubator. Phase contrast images and fluorescence images of cells transfected with pAAV-GFP for 48 h were collected at equal exposure conditions under Nikon Eclipse Ti microscopy (magnification ×100) with NIS-Elements BR 3.0 software (Nikon).

### Western Blotting

Cells (or mouse pancreas) were lysed in radioimmunoprecipitation assay buffer 48 h after transfection. The lysates were directly subjected to SDS-PAGE followed by Western blotting with antibody against Klotho (R&D Systems), Rac1, and p-Rac1 as we described previously (20,21). The blot was rinsed and reprobed with antibody against β-actin or α-tubulin for loading controls.

### Animal Study Protocol

This study was carried out in accordance with the National Institutes of Health (NIH) Guide for the Care and Use of Laboratory Animals. This project was approved

by the Institutional Animal Care and Use Committee at the University of Oklahoma Health Sciences Center.

Eight-week-old male BKS.Cg-+*Lepr*$^{db}$/+*Lepr*$^{db}$/OlaHsd (*db/db*) mice and BKS.Cg-*Dock*$^{7m}$+/+*Lepr*$^{db}$/OlaHsd (lean) mice were purchased from Harlan Laboratories (Indianapolis, IN). All mice were housed in cages at room temperature (25 ± 1°C) and provided with Purina laboratory chow (No. 5001) and tap water ad libitum throughout the experiment. Three groups of *db/db* mice and three groups of lean mice were used (7–8 mice/group). Body weight was monitored weekly. Blood glucose was measured weekly from tail vein blood using a ReliOn Ultima glucose reader (Solartek Products, Inc., Alameda, CA). The mice were fasted for 12 h before glucose measurement. PBS, rAAV-GFP, or rAAV-mKL were carefully injected intraperitoneally into the region of pancreas of lean and *db/db* mice (10 weeks) at the dose of $2.57 \times 10^9$ of viral genome copies/g body weight in a total volume of 500 μL.

### Glucose Tolerance Test and Insulin Sensitivity Test

The glucose tolerance test (GTT) was performed during weeks 2, 4, and 6 after the treatments. The insulin sensitivity test (IST) was performed during weeks 3 and 5 after the treatments. Briefly, blood glucose levels were measured at 30, 60, 90, and 120 min after subcutaneous injections of D-glucose 1 g/kg (Fisher Scientific) or insulin 1.0 unit/kg (Sigma-Aldrich). The baseline glucose levels were determined after a 12-h fast.

### Tissue Collection

At the end of week 6 of the treatments, five animals from each treatment group were killed with an overdose of sodium pentobarbital (100 mg/kg i.p.), and blood was collected in EDTA. The plasma samples were stored at −80°C. After blood collection, animals were perfused transcardially with heparinized saline. One-fifth of the pancreas was embedded in optimal cutting temperature compound (Tissue-Tek) on dry ice and stored at −80°C until use. The rest of the pancreas was fixed in 4% PBS-buffered paraformaldehyde for 24 h and then embedded in paraffin.

For preliminary experiments, 20-week-old male *db/db* and lean mice were purchased from Harlan Laboratories (Indianapolis, IN). Four to five animals from each stain were killed with an overdose of sodium pentobarbital (100 mg/kg i.p.). The animals were perfused transcardially with heparinized saline. One-fourth of the pancreas was used for Western blot analysis of Klotho protein expression. The rest of the pancreas was fixed in 4% PBS-buffered paraformaldehyde for 24 h and then embedded in paraffin for immunohistochemical (IHC) analysis of Klotho and insulin protein expression. A total of 20–25 islets were examined for each mouse.

### Pancreatic Islet Isolation

At the end of week 6 of the treatments, three animals from each treatment group were sacrificed. Mouse pancreatic islets were isolated using a modified protocol as described previously (22). Briefly, collagenase P was injected into the common bile duct of a mouse. The pancreas was then excised and digested at 37°C. The islets were first purified with premixed Histopaque gradient and then purified by handpicking the separated islets with low-retention pipette tips under a dissecting microscope. When viewed under the microscope, spherical and golden-brown particles (darker color) with diameters of 100–300 μm were considered islets. Five size-matched islets from each animal were cultured with RPMI1640 with 10% FBS in a 24-well plate overnight. The rest of the isolated islets were stored at −80°C until use.

### Glucose-Stimulated Insulin Secretion

After overnight incubation in 10% FBS RPMI1640, the isolated islets were starved with Krebs-Ringer bicarbonate (125 mmol/L NaCl, 4.74 mmol/L KCl, 1 mmol/L $CaCl_2$, 1.2 mmol/L $KH_2PO_4$, 1.2 mmol/L $MgSO_4$, 5 mmol/L $NaHCO_3$, and 25 mmol/L HEPES; pH 7.4) supplemented with 0.1% BSA and 2.8 mmol/L glucose for 1 h. Islets were washed with PBS and incubated with Krebs-Ringer bicarbonate buffer supplemented with 2.8 or 16.7 mmol/L glucose for 1 h. Medium was collected and stored at −80°C for measuring insulin levels.

### Insulin Measurement

Insulin levels in plasma or supernatants from glucose-treated islets were measured using an insulin enzyme immunosorbent assay kit according to the manufacturer's instructions (ALPCO Diagnostics, Salem, NH).

### Immunohistochemistry

A series of 5-μm–thick sections of paraffin-embedded pancreas were cut at 100-μm intervals on three levels. For IHC analysis, consecutive pancreatic cross sections were deparaffinized, rinsed in xylene, and rehydrated. After heat-induced antigen retrieval in a microwave, the cross sections were blocked first with 3% hydrogen peroxide. The sections were incubated with antibodies against GFP (ab290; Abcam), Flag-tag (ET-DY100; Aves Labs), Klotho (R&D Systems), insulin (sc-9168; Santa Cruz Biotechnology), Pdx-1 (AB3503; Millipore), 4-hydroxyonenal (4-HNE) (ab48506; Abcam), DnaJ (Hsp40) homolog C3 (DNAJC3) (ab70840; Abcam), proliferating cell nuclear antigen (PCNA) (ab2426; Abcam), or microtubule-associated protein 1 light chain 3 (LC3) (L1564-50A; United States Biological) overnight at 4°C and then with appropriated secondary antibodies conjugated with horseradish peroxidase at room temperature for 60 min. Stable diaminobenzidine (Invitrogen) was used as a substrate for peroxidase. Hematoxylin was used as counterstaining. The islets of Langerhans in the cross sections of pancreas for each mouse were located under a microscope (Nikon Eclipse Ti). Images of islets from consecutive cross sections for each animal were collected at equal exposure conditions and at the same magnification (40× objective lens). The staining for Klotho, insulin, Pdx-1, or LC3 was quantified using NIH ImageJ freeware as mean gray value/pixel. Briefly, the selection line was drawn along the islet of Langerhans after the original red, green, and blue image was converted to a gray

scale image. A TUNEL assay on the cross sections of mouse pancreas was performed using TACS XL Blue Label In Situ Apoptosis Detection Kit (Trevgen, Gaithersburg, MD). The number of cells with positive insulin, 4-HNE, DNAJC3, TUNEL, or PCNA staining in the islet was counted by NIS-Elements BR 3.0 software. A total of 20–25 islets were examined for each animal.

### In Situ Measurement of Superoxide

Dihydroethidium (DHE) (D7008; Sigma-Aldrich) was used to measure superoxide levels in pancreatic islets as we described previously (15,20,21,23,24). Briefly, 6-μm–thick cross sections of frozen optimal cutting temperature compound-embedded pancreas were cut on a cryomicrotome and fixed with 4% paraformaldehyde for 10 min. DHE 2.5 μmol/L was added to the sections and incubated at 37°C for 20 min. Fluorescence images of ethidium-stained islets for each sample were collected at equal exposure conditions under Nikon Eclipse Ti microscopy (magnification ×400) with NIS-Elements BR 3.0 software. The mean fluorescence density of pancreatic islets (20–25 islets/mouse) was also analyzed with NIS-Elements BR 3.0 software.

### RNA Isolation and Real-Time RT-PCR

Total RNA was purified from isolated mouse pancreatic islets using TRIzol Reagent followed by QIAGEN RNeasy Mini Kit. RNA (2 μg) was reverse transcribed using SuperScript III Reverse Transcriptase with random hexamer in the presence of 10 μL deoxyribonucleotide for 1 h at 50°C. The resulting cDNAs were used as templates for real-time PCR, with oligonucleotides primers used to amplify the mRNAs of *insulin I* (F: 5′-CCTGTTGGTG CACTTCCTAC-3′; R: 5′-TGCAGTAGTTCTCCAGCTGG-3′; size: 317 bp), *insulin II* (F: 5′-AGCCCTAAGTGATCCGCT ACAA-3′; R: 5′-CATGTTGAAACAATAACCTGGAAGA-3′; size: 178 bp), *Pdx-1* (F: 5′-CCACCCCAGTTTACAAG CTC-3′; R: 5′-ACGGGTCCTCTTGTTTTCCT-3′; size: 315 bp), *DNAJC3* (F: 5′-AAGCCCGTGGAAGCCATTAG-3′; R: 5′-GGTCATTTTCATTGTGCTCCTGAG-3′; size: 160 bp), *PCNA* (F: 5′-TAAAGAAGAGGAGGCGGTAA-3′; R: 5′-TAAG TGTCCCATGTCAGCAA-3′; size: 175 bp), *LC3* (F: 5′-CGAG CGCTACAAGGGTGAG-3′; R: 5′-CCGGATGATCTTGAC CAAC-3′; size: 100 bp), and *β-actin* (F: 5′-AGGTCAT CACTATTGGCAACGA-3′; R: 5′-CACTTCATGATGGAAT TGAATGTAGTT-3′; size: 118 bp) (25–29). Real-time PCR was performed on a Bio-Rad CFX96 Real-Time PCR Detection System. PCRs were cycled 40 times under the following conditions: 95°C for 5 s and 58°C for 5 s. Homogeneity of PCR products from each reaction was confirmed by melt curve analysis and 1.5% agarose gel analysis.

### Statistical Analysis

Data from collected human and mouse Klotho and insulin in pancreases were analyzed using the unpaired *t* test. Blood glucose and body weight were analyzed by a repeated-measures one-way ANOVA. The remaining data were analyzed by one-way ANOVA. The Newman-Keuls procedure was used to reveal differences between groups. $P < 0.05$ was considered to be statistically significant.

## RESULTS

### Klotho Was Depleted in Pancreatic Islets in T2DM Patients and Diabetic Mice

We performed IHC staining of Klotho and insulin in human pancreas. Both Klotho and insulin staining were significantly decreased in pancreatic islets of patients with T2DM versus those of healthy donors (Fig. 1*A* and *B*). We further quantified Klotho protein expression levels in human pancreas using Western blot. Klotho protein expression was significantly decreased in pancreas in patients with T2DM (Fig. 1*C*).

We next assessed Klotho expression in pancreata in a mouse model of T2DM (*db/db* mice). The IHC analysis showed a significant decrease in Klotho protein expression in pancreatic islets in *db/db* mice (Fig. 1*D* and *E*). The insulin storage was also significantly decreased in pancreatic islets in *db/db* mice compared with lean mice (Fig. 1*D* and *E*). We previously reported that Klotho protein is expressed in mouse pancreatic islets of Langerhans with an apparent molecular weight of 65 kDa (11). Western blot analysis indicated that Klotho protein expression levels were significantly decreased in pancreas of *db/db* mice (20 weeks) versus age-matched lean mice (Fig. 1*F*). These results indicate that downregulation of Klotho protein expression is associated with a decrease in insulin storage in pancreatic β-cells in patients with T2DM and in *db/db* mice.

### β-Cell–Specific Expression of mKL In Vitro

To test the β-cell specificity of the mouse *insulin II* promoter, we transfected MIN6 β-cells, 3T3-L1 preadipocytes, and mIMCD3 cells with 0.072 μg/mL pAAV-GFP, pAAV-mKL, or pAAV-CMV-mKL DNAs for 48 h. In pAAV-GFP and pAAV-mKL, the original *CMV* promoter was replaced by the mouse *insulin II* promoter. pAAV-GFP (GFP protein) was specifically expressed in MIN6 cells but not in 3T3-L1 or mIMCD3 cells (Supplementary Fig. 1*A*), indicating that the *insulin II* promoter is β-cell specific. The constructed *insulin II* promoter and the conventional *CMV* promoter are equally potent in driving *mKL* expression in MIN6 β-cells (Supplementary Fig. 1*B*).

### β-Cell–Specific Expression of mKL Attenuated the Development of Diabetes in *db/db* Mice

We carefully injected rAAV-GFP or rAAV-mKL into the region of pancreas intraperitoneally in lean and *db/db* mice. These *db/db* mice were developing severe hyperglycemia at the age of 10 weeks (Fig. 2*A*). Of note, rAAV-mKL significantly attenuated hyperglycemia and dampened the development of overt diabetes in *db/db* mice within 2 weeks compared with the PBS- and rAAV-GFP–treated control groups (Fig. 2*A*). The antihyperglycemic effects of rAAV-mKL were sustained for 6 weeks (length of the study), although it did not eventually prevent the rise of blood glucose levels (Fig. 2*A*). The rAAV-mKL did not alter blood glucose levels significantly in lean mice (Fig. 2*A*).

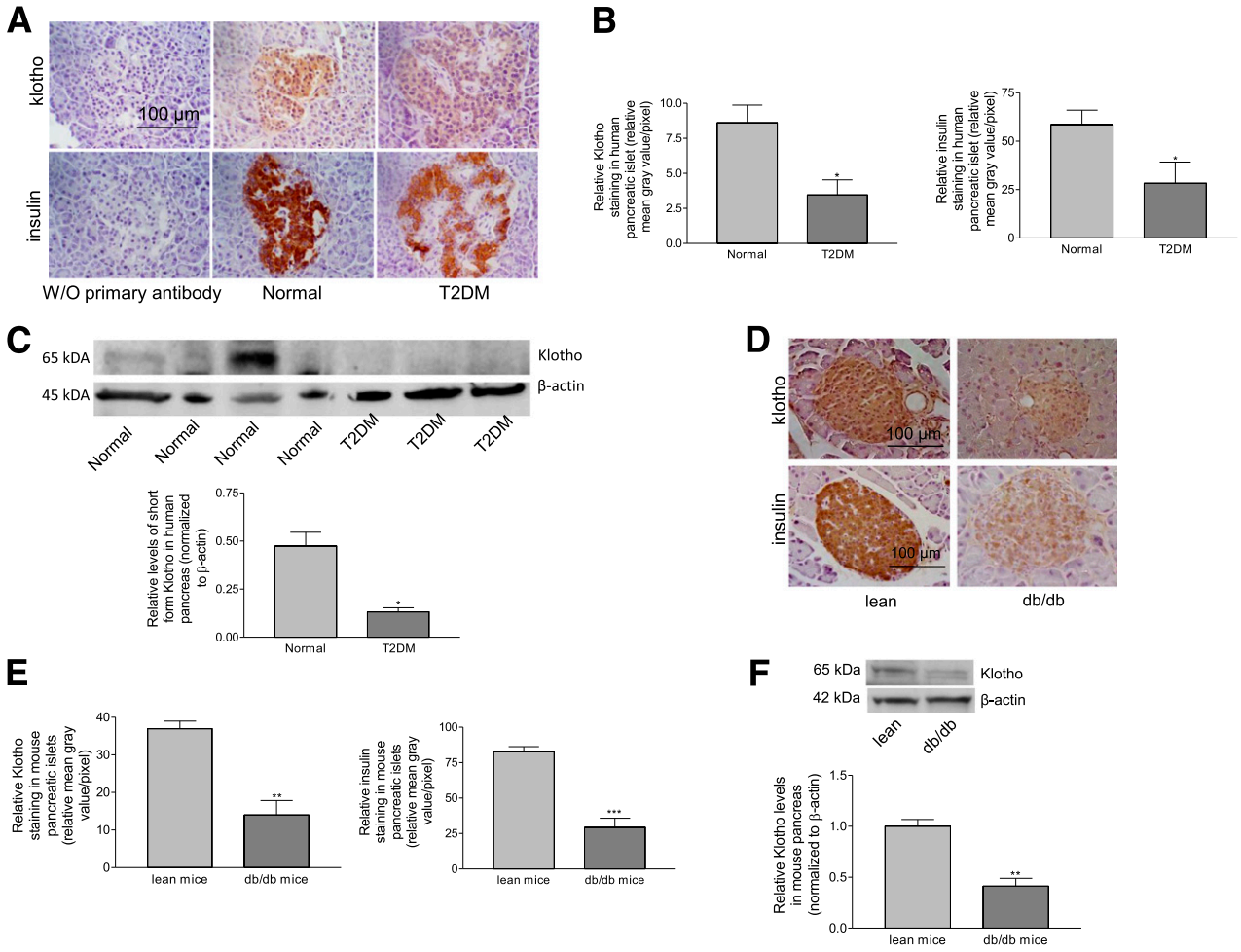


**Figure 1**—Expressions of Klotho in pancreatic islets of T2DM patients and *db/db* mice (20 weeks old). *A*: Representative images of Klotho and insulin staining (brown) in cross sections of human pancreatic islets. *B*: Semiquantification of Klotho and insulin staining in human pancreatic islets. $n = 4–6$. $^*P < 0.05$ vs. the normal samples. *C*: Western blot analysis of Klotho protein expression in human pancreas. Results were standardized to β-actin. $n = 3–4$. $^*P < 0.05$ vs. the normal samples. *D*: Representative images of Klotho and insulin staining (brown) in cross sections of mouse pancreatic islets. *E*: Semiquantification of Klotho and insulin staining in mouse pancreatic islets. $n = 4–5$. $^{**}P < 0.01$, $^{***}P < 0.001$ vs. the lean mice. *F*: Western blot analysis of Klotho protein expression in mouse pancreas. Results were standardized to β-actin vs. the lean mice. $n = 4–5$. $^{**}P < 0.01$ vs. the lean mice. W/O, without.

To gain insight into the mechanism of the Klotho action, we performed a GTT at weeks 2, 4, and 6 and an IST at weeks 3 and 5 following Klotho gene delivery. The *db/db* mice showed overt glucose intolerance versus the lean mice (Fig. 2*B–D*). Treatments with rAAV-mKL markedly improved glucose tolerance in *db/db* mice, and glucose tolerance was not altered by rAAV-mKL in lean mice (Fig. 2*B–D*). The *db/db* mice developed severe insulin resistance; however, β-cell–specific expression of Klotho did not affect insulin sensitivity in either *db/db* or lean mice (Fig. 2*E* and *F*). These data suggest that the treatments with rAAV-mKL improved β-cell function but did not affect insulin sensitivity in peripheral tissues in diabetic mice.

The *db/db*-PBS group exhibited slightly higher levels of plasma insulin compared with the lean-PBS group (Fig. 2*G* and *H*). rAAV-mKL further increased plasma insulin levels significantly in *db/db* mice but not in lean mice (Fig. 2*G* and *H*). These results suggest that rAAV-mKLs increase insulin release in response to hyperglycemia in *db/db* mice.

Fasting urine glucose levels in *db/db* mice were significantly higher than those of lean mice. rAAV-mKL significantly decreased urine glucose levels in *db/db* mice at weeks 2 and 4 after gene delivery (Fig. 2*I*).

### Effects of β-Cell–Specific Expression of mKL on Body Weight, Food Intake, Water Intake, and Urine Output in Diabetic Mice

The control *db/db* mice had much greater body weights than the control lean mice (Supplementary Fig. 2*A*). β-Cell–specific delivery of mKL did not affect the body weights significantly in either lean or *db/db* mice (Supplementary Fig. 2*A*). The rAAV-mKL slightly but significantly decreased food intake in *db/db* mice (normalized to body weight) at week 5 after gene delivery (Supplementary Fig.

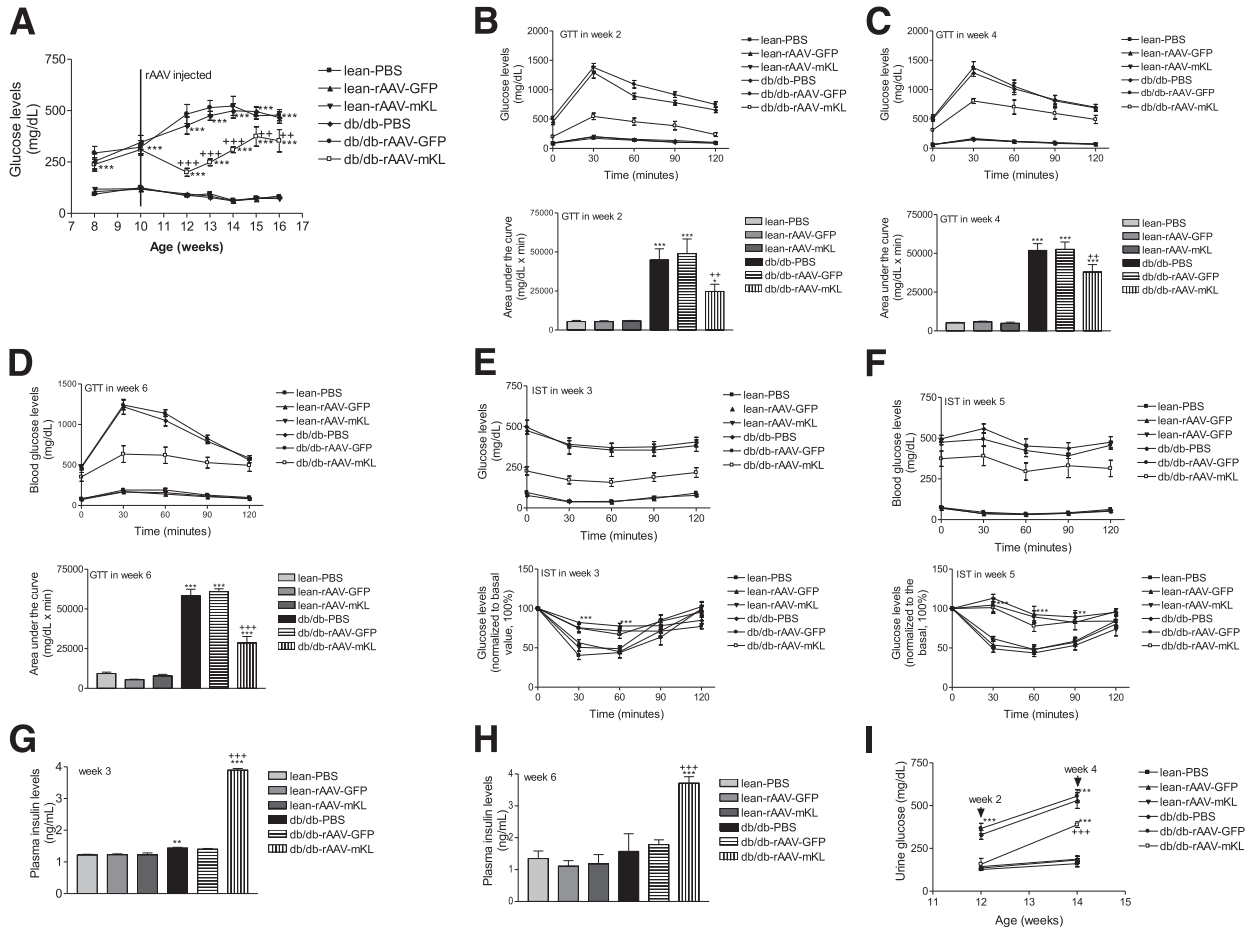


**Figure 2—**Effects of the β-cell–specific expression of mKL on blood glucose levels, glucose tolerance, insulin sensitivity, and plasma insulin levels in diabetic mice. Time course of fasting blood glucose levels (*A*). GTT results at week 2 (*B*), week 4 (*C*), and week 6 (*D*) after gene delivery. IST results at week 3 (*E*) and week 5 (*F*) after the treatments. Plasma insulin levels at week 3 (*G*) and week 6 (*H*) after gene delivery. Urine glucose levels at week 2 and 4 after gene delivery (*I*). Data are mean ± SEM. $n$ = 6–8 animals/group (except for plasma samples where $n$ = 3–5 animals/group). *$P$ < 005, **$P$ < 0.01, ***$P$ < 0.001 vs. the lean-PBS group; ++$P$ < 0.01, +++$P$ < 0.001 vs. the *db/db*-PBS group.

2*B–D*). The control *db/db*-PBS group had greater water intake and urine output than the lean mice (Supplementary Fig. 2*E–J*). The rAAV-mKL attenuated both water intake and urine output in diabetic mice at weeks 3 and 5 after gene delivery (Supplementary Fig. 2*E–J*).

### IHC and Functional Analysis of Mouse Pancreatic Islets of Langerhans

Different serotypes of rAAV with single- or double-stranded DNA have been used in pancreatic islet gene transfer with various efficiencies through different routes (16,30,31). Given that the insert genes ranged from 0.7 to 3.1 kilobases, AAV2 vector with single-stranded DNA was used in the gene transfer. A FLAG-tag sequence was inserted at the 3′ end of the mouse *Klotho* gene. At 6 weeks after gene delivery, we first examined GFP and FLAG-tag protein expression in cross sections of paraffin-embedded pancreatic islets, livers, and kidneys through IHC analysis. The rAAV-GFP drove *GFP* expression in pancreatic islets of lean and *db/db* mice, whereas GFP was not detectable in the livers and kidneys of animals injected with rAAV-GFP (Supplementary Fig. 3*A* and *B*). In addition, rAAV-mKL drove FLAG-tag expression in islets of animals treated with rAAV-mKL (Supplementary Fig. 3*C*). Thus, the intraperitoneal delivery of rAAV coupled with mouse *insulin II* promoter led to islet-specific gene transfer in mice.

We next studied Klotho expression in pancreatic islets in diabetic mice. Klotho staining in pancreatic islets of Langerhans in control *db/db* mice was significantly decreased compared with that of control lean mice (Fig. 3*A* and *B*). The treatments with rAAV-mKL increased Klotho staining in pancreatic islets of both lean and *db/db* mice (Fig. 3*A* and *B*). Western blot analysis also showed that the treatments with rAAV-mKL increased Klotho protein expression in pancreas of lean and *db/db* mice (Supplementary Fig. 3*D* and *E*).

To investigate whether the β-cell–specific expression of mKL exerts beneficial effects on pancreatic islets of Langerhans, we performed insulin staining in pancreatic cross sections. Insulin staining in pancreatic islets was significantly decreased in *db/db* mice compared with that of lean

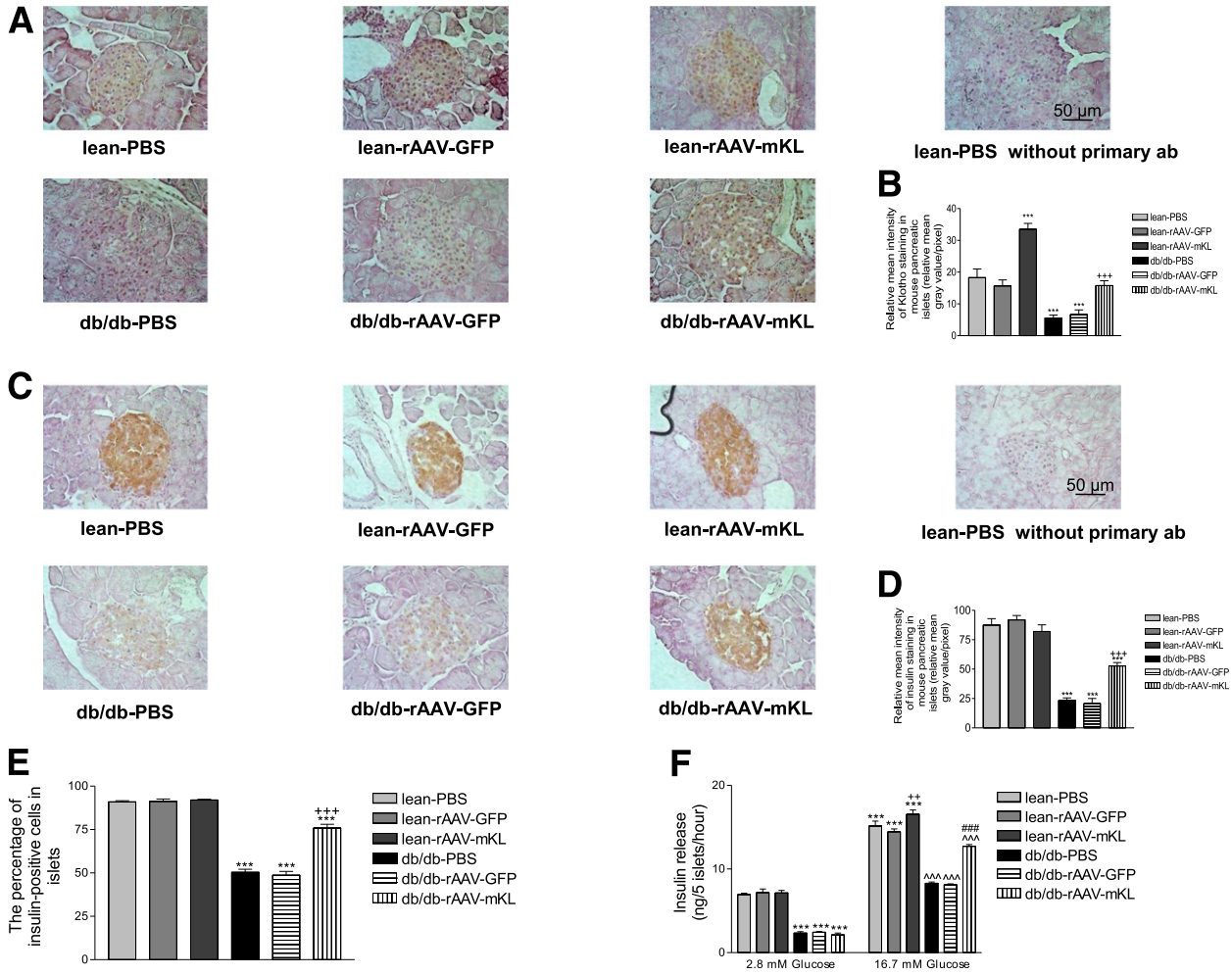


**Figure 3—**Expressions of Klotho and insulin in pancreatic islets and analysis of the islet function in diabetic mice. Animals were sacrificed 6 weeks after gene delivery. *A*: Representative images of Klotho staining (brown) in cross sections of mouse pancreatic islets. *B*: Semiquantification of Klotho staining in pancreatic islets ($n$ = 4–5). *C*: Representative images of insulin staining (brown) in cross sections of islets. *D*: Semiquantification of insulin staining in pancreatic islets ($n$ = 4–5). *E*: The percentage of insulin-positive cells in pancreatic islets ($n$ = 4–5). ***$P$ < 0.001 vs. the lean-PBS group, +++$P$ < 0.001 vs. the *db*/*db*-PBS group. *F*: Glucose-stimulated insulin secretion from pancreatic islets. Isolated islets were stimulated with 2.8 or 16.7 mmol/L glucose. Insulin levels in the medium were measured. Data are mean ± SEM. $n$ = 3 animals/group. ***$P$ < 0.001 vs. the lean-PBS group treated with 2.8 mmol/L glucose, ^^^$P$ < 0.001 vs. the *db*/*db*-PBS group treated with 2.8 mmol/L glucose, ###$P$ < 0.001 vs. the *db*/*db*-PBS group treated with 16.7 mmol/L glucose, ++$P$ < 0.01 vs. the lean-PBS group treated with 16.7 mmol/L glucose. ab, antibody.

mice (Fig. 3*C* and *D*). Of note, β-cell–specific expression of mKL increased insulin staining in pancreatic islets of *db/db* mice by 1.26-fold (Fig. 3*D*). In addition, the number of insulin-positive cells in pancreatic islets of Langerhans in *db/db* mice was significantly less than that of lean mice (Fig. 3*E*). In contrast, β-cell–specific expression of mKL partially restored the number of insulin-positive cells in pancreatic islets in *db/db* mice (by 55%) (Fig. 3*E*).

We further tested the glucose-stimulated insulin secretion in isolated mouse pancreatic islets (ex vivo). Insulin secretion was lower at both 2.8 and 16.7 mmol/L glucose in islets isolated from *db/db* mice compared with that of lean mice (Fig. 3*F*). β-Cell–specific expression of mKL promoted insulin secretion in response to 16.7 mmol/L glucose but not 2.8 mmol/L glucose in islets of lean and *db/db* mice (Fig. 3*F*). These results reveal, for the first time, that the pancreatic islets of *db/db* mice lose compensatory ability in response to increased blood glucose levels and that β-cell–specific expression of mKL improves the impaired response of pancreatic β-cells to glucose challenge in *db/db* mice.

### Effects of β-Cell–Specific Expression of mKL on Oxidative Stress, Superoxide Levels, and Pdx-1 Expression in Pancreatic Islets of *db/db* Mice

To study the mechanisms for the preservation of β-cell function by Klotho in *db/db* mice, we evaluated oxidative stress markers (4-HNE), intracellular superoxide (DHE staining), and insulin transcription factors (Pdx-1) in pancreatic islets. The number of 4-HNE–positive cells and the intracellular superoxide level were significantly increased in pancreatic islets of *db/db* mice (Fig. 4*A–D*), indicating

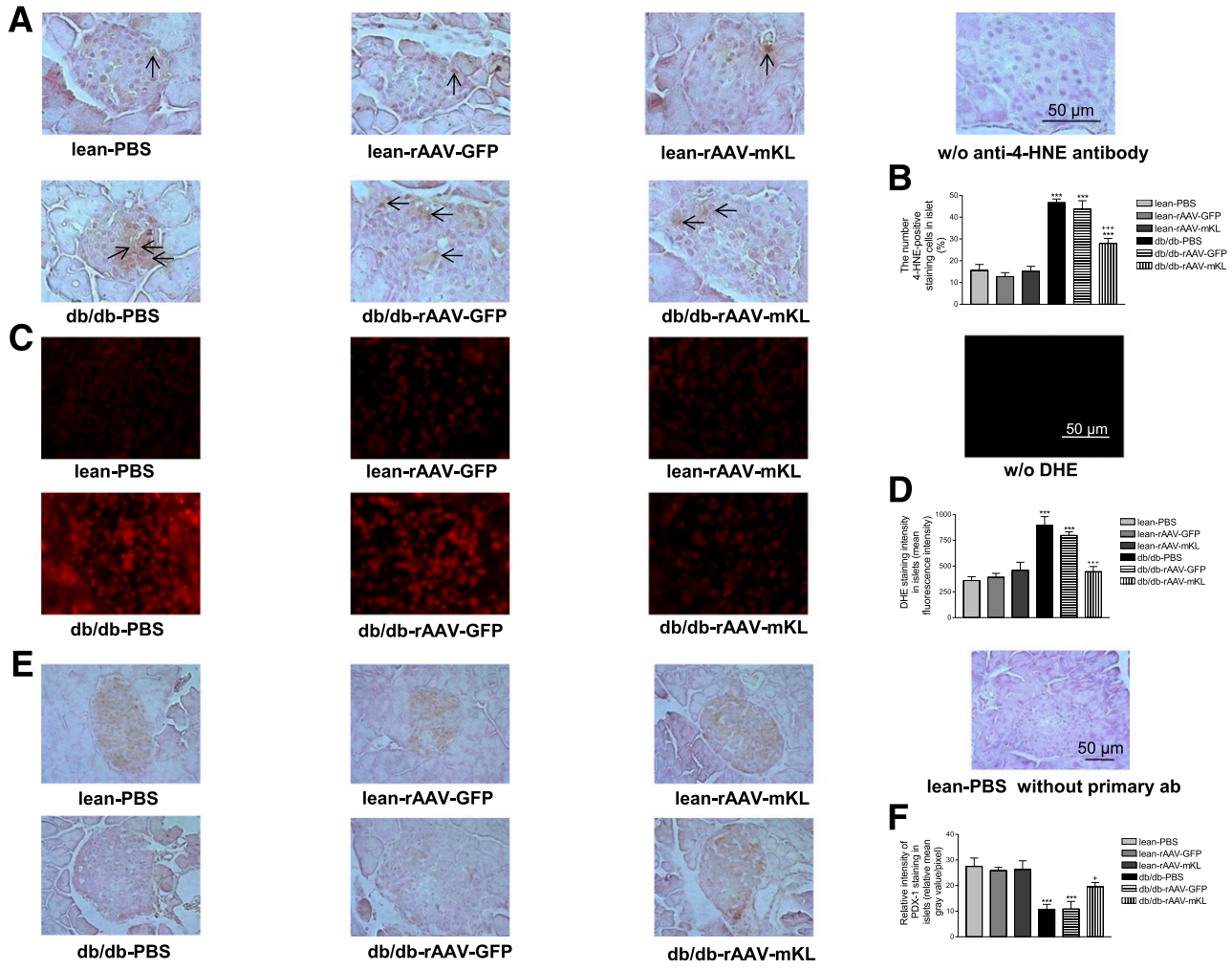


**Figure 4**—Oxidative stress, superoxide, and Pdx-1 levels in pancreatic islets of diabetic mice. *A*: Representative images of 4-HNE staining (brown, indicated by arrows) in cross sections of mouse pancreatic islets. *B*: The percentage of 4-HNE–positive cells in pancreatic islets. *C*: Representative images of DHE staining (red) in pancreatic islets. *D*: Quantification of superoxide levels (DHE staining) in pancreatic islets. *E*: Representative images of Pdx-1 staining in pancreatic islets. *F*: Semiquantification of Pdx-1 staining in pancreatic islets. Data are mean ± SEM. $n$ = 4–5 animals/group. ***$P < 0.001$ vs. the lean-PBS group; +$P < 0.05$, +++$P < 0.001$ vs. the *db/db*-PBS group. ab, antibody; w/o, without.

oxidative damage. In vivo expression of mouse Klotho attenuated the oxidative stress levels in pancreatic islets of *db/db* mice (Fig. 4*A*–*D*). In addition, the Pdx-1 expression level (staining) was significantly lower in pancreatic islets of *db/db* animals, whereas β-cell–specific expression of mKL increased Pdx-1 in islets of *db/db* mice (Fig. 4*E* and *F*). Thus, the beneficial effects of Klotho on β-cells may involve suppression of oxidative stress and enhancement of Pdx-1 expression in diabetic mice.

### Effects of β-Cell–Specific Expression of mKL on DNAJC3, LC3, Cell Proliferation, and Apoptosis in Pancreatic Islets of *db/db* Mice

Because oxidative stress could damage cells, we further assessed the endoplasmic reticulum (ER) stress marker DNAJC3, autophagy marker LC3, cell proliferation, and cell apoptosis in pancreatic islets in diabetic mice. The number of DNAJC3-positive cells in the pancreatic islets was significantly increased in *db/db* mice versus lean mice. In contrast, β-cell–specific expression of mKL decreased the number of DNAJC3-positive cells in islets of *db/db* mice, suggesting that expression of Klotho suppresses ER stress in islets of *db/db* mice (Fig. 5*A* and *B*). LC3 staining was lower in islets of *db/db* mice compared with that of lean mice, suggesting that the autophagic activity was decreased in pancreatic islets of *db/db* mice. Of note, β-cell–specific expression of mKL restored autophagic activity in *db/db* mice (Fig. 5*C* and *D*).

On the other hand, the number of PCNA-positive cells in islets was increased in *db/db* mice compared with lean mice, and β-cell–specific expression of Klotho further increased the number of PCNA-positive cells in islets of *db/db* mice (Fig. 6*A* and *B*). Therefore, in vivo expression of Klotho further promoted cell proliferation in pancreatic

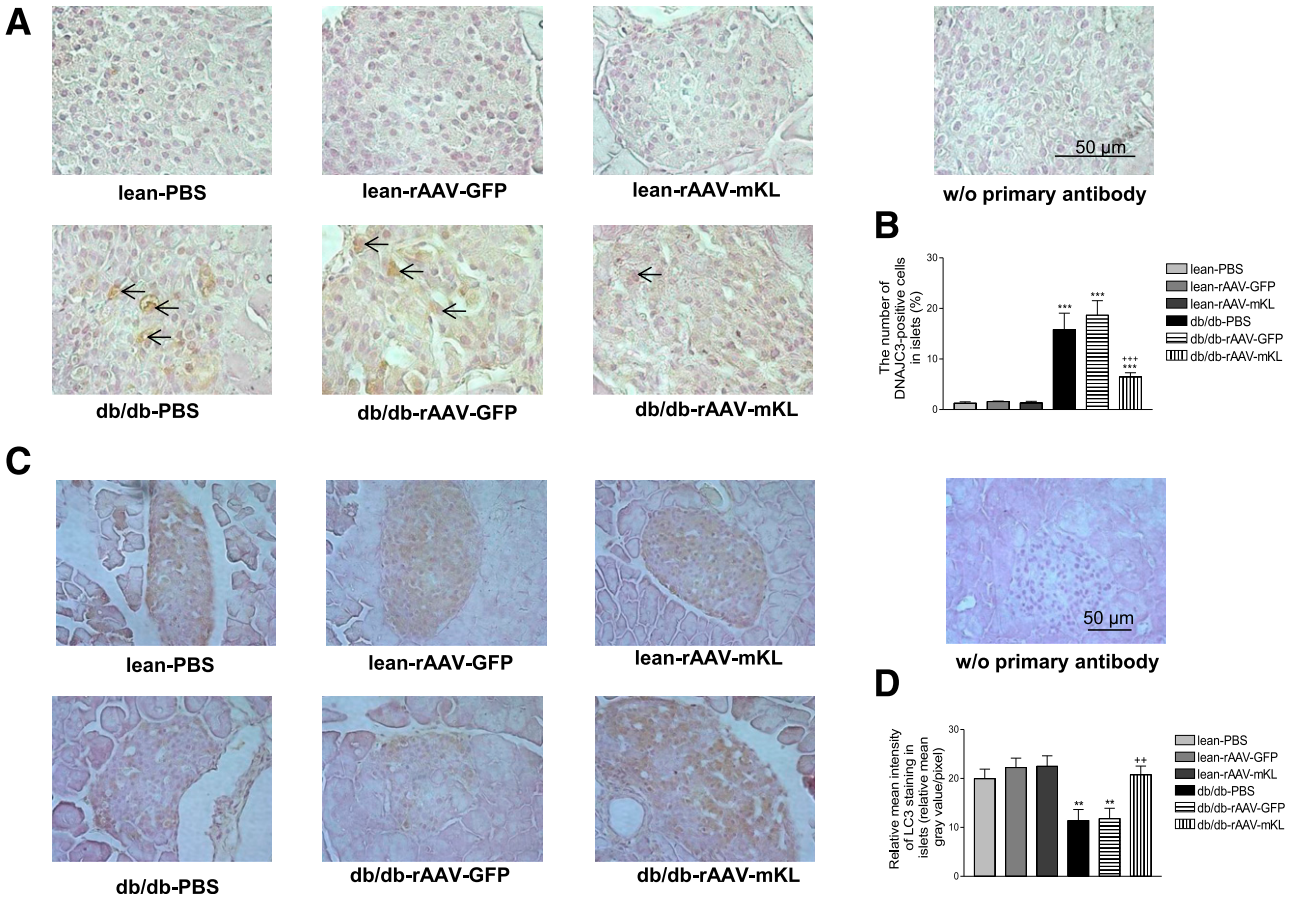


**Figure 5—**Effects of β-cell–specific expression of mKL on ER stress and autophagy in pancreatic islets. *A*: Representative images of DNAJC3 staining (brown, indicated by arrows) in mouse pancreatic islets. *B*: The percentage of DNAJC3-positive–staining cells in pancreatic islets. *C*: Representative images of LC3 staining (brown) in cross sections of mouse pancreatic islets. *D*: Semiquantification of LC3 staining in pancreatic islets. Data are mean ± SEM. $n$ = 4–5 animals/group. $^{**}P < 0.01$, $^{***}P < 0.001$ vs. the lean-PBS group; $^{++}P < 0.01$, $^{+++}P < 0.001$ vs. the *db/db*-PBS group. w/o, without.

islets of *db/db* mice. The number of apoptotic cells was increased in islets of *db/db* mice, which can be dampened by expression of Klotho (Fig. 6*C* and *D*). Thus, rAAV-mKL treatments attenuated apoptosis in pancreatic islets of *db/db* mice (Fig. 6*C* and *D*). Therefore, the preservation of β-cell function in *db/db* mice may be partially attributed to suppression of ER stress and apoptosis, restoration of autophagic activity, and enhancement of β-cell proliferation.

### Effects of β-Cell–Specific Expression of mKL on Gene Expression in Islets of Diabetic Mice

We also assessed whether Klotho affects the corresponding gene expressions in line with the changes in several proteins involved in the preservation of pancreatic islets. The *db/db* mice exhibited significantly lower mRNA expression levels of *insulin I*, *insulin II*, *Pdx-1*, and *LC3*, whereas the treatments with rAAV-mKL increased mRNA levels of these genes in islets of diabetic mice (Fig. 7*A*–*D*). In addition, *db/db* mice had higher mRNA expression levels of *DNAJC3* and *PCNA*, whereas the rAAV-mKL treatments decreased *DNAJC3* mRNA expression but further increased *PCNA* mRNA expression levels in islets (Fig. 7*E* and *F*). These data suggest that β-cell–specific expression of mKL preserves β-cells through regulating the gene expression of *insulin I*, *insulin II*, *Pdx-1*, *PCNA*, and *LC3* mRNA.

### Effects of Overexpression of mKL on NADPH Oxidase Activity, Superoxide Production, p-Rac1, and Rac1 in MIN6 β-Cells Treated With High Glucose

Because the beneficial effects of Klotho on β-cells involved suppression of superoxide production and oxidative stress (Fig. 4*A*–*D*), we further investigated the underlying mechanism in MIN6 β-cells. High glucose levels increased the activity of NADPH oxidases (Fig. 8*A*), an important source of superoxide in MIN6 β-cells. Of note, overexpression of mKL abolished high glucose–induced activation of NADPH oxidases and superoxide production in MIN6 β-cells (Fig. 8*A*–*C*), suggesting that the NADPH oxidase is involved in the upregulation of superoxide generation. Furthermore, overexpression of mKL eliminated high glucose–induced activation of Rac1 (p-Rac1) without altering the total

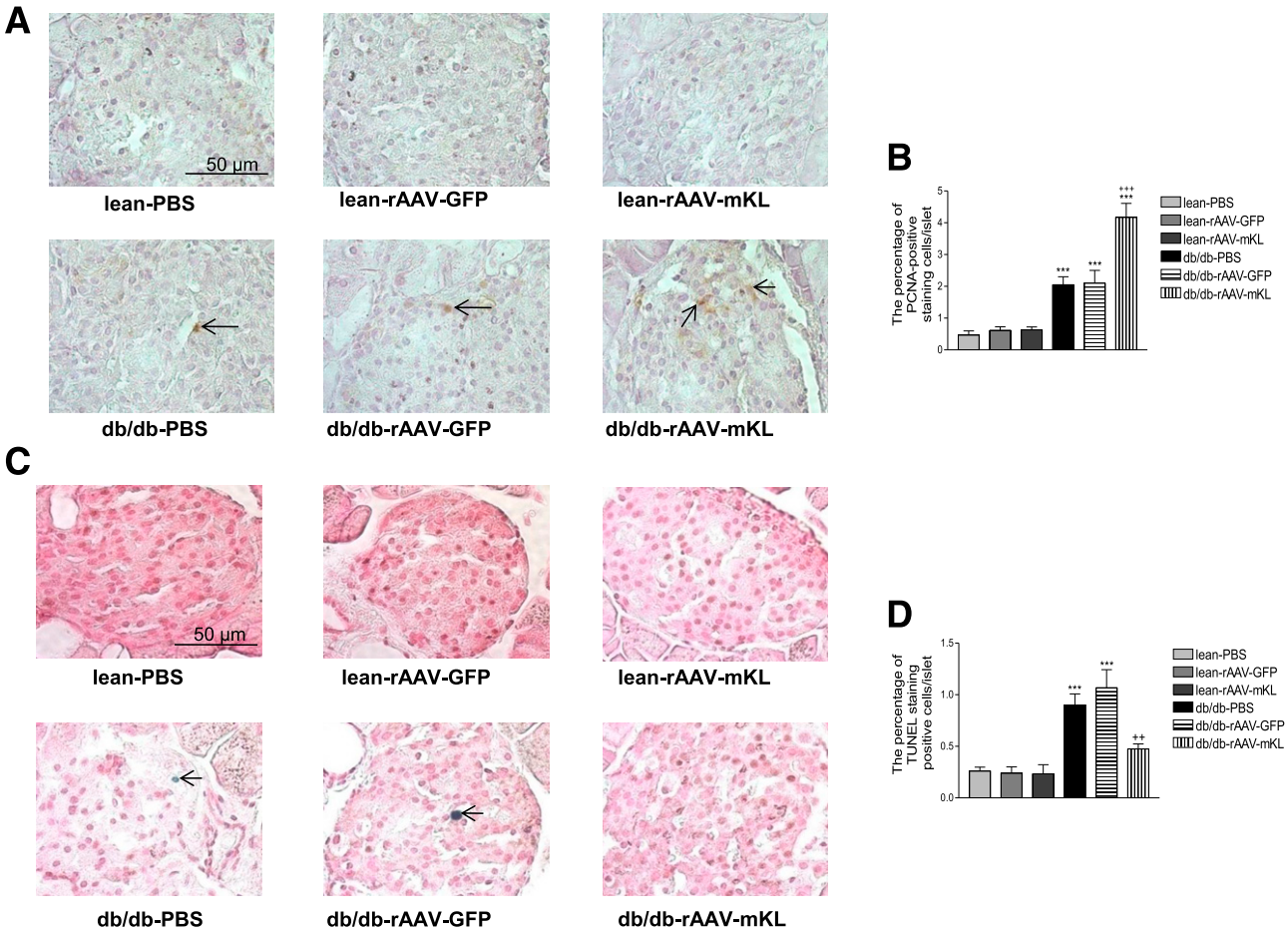


**Figure 6**—Effects of β-cell–specific expression of mKL on cell proliferation and apoptosis in pancreatic islets. *A*: Representative images of PCNA staining (indicated by arrows, brown) in mouse pancreatic islets. *B*: The percentage of PCNA-positive cells in pancreatic islets. *C*: Representative images of TUNEL staining (indicated by arrows, blue) in pancreatic islets. *D*: The percentage of TUNEL-positive apoptotic cells in pancreatic islets. Data are mean ± SEM. $n$ = 4–5 animals/group. ***$P$ < 0.001 vs. the lean-PBS group; ++$P$ < 0.01, +++$P$ < 0.001 vs. the *db/db*-PBS group.

Rac1 level (Fig. 8*D–F*), a key regulator of the NADPH oxidase activity. These results suggest that the suppressor effect of mKL on NADPH oxidase activity is mediated by inhibition of Rac1 phosphorylation.

We next assessed the subcellular localization of the short-form Klotho (65 kDa) using confocal microscopy. Endogenous 65-kDa Klotho (red) was found in the cytosol and nucleus (Supplementary Fig. 4*A*). Our previous study indicated that the short-form Klotho is also expressed in the plasma membrane (11), although the current IHC method could not show its membrane localization. The transgene-expressed Klotho detected using FLAG-tag staining (green) was located in the cytosol and outside the nucleus (Supplementary Fig. 4*B*).

### Effects of Short-Form and Full-Length Klotho Protein on Glucose-Induced Insulin Release in Isolated β-Islets

We further assessed the effects of recombinant short-form Klotho (65 kDa) and full-length Klotho (130 kDa) protein on β-cell function in the β-islets isolated from lean mice. The β-islets were treated with 65- and 130-kDa Klotho proteins. We found that only short-form Klotho promoted insulin secretion in β-islets (Supplementary Fig. 5). The full-length Klotho did not have obvious effects on insulin secretion in β-islets (Supplementary Fig. 5). Exogenous short-form Klotho could bind to the cell membrane. We demonstrated previously that short-form Klotho in the cell membrane enhances glucose-induced insulin secretion by upregulating membrane levels of transient receptor potential V2 (TRPV2), which increases glucose-induced calcium responses (11).

## DISCUSSION

Pancreatic β-cells are essential to the regulation of glucose homeostasis. Substantial β-cell failure is now believed to occur at an early stage in the progression of T2DM (2). Thus, one of the goals in the treatment of T2DM is to preserve functional β-cells. *Klotho*, a recently discovered aging-suppressor gene, was believed to be expressed in kidneys (21). Our most recent study indicates that the

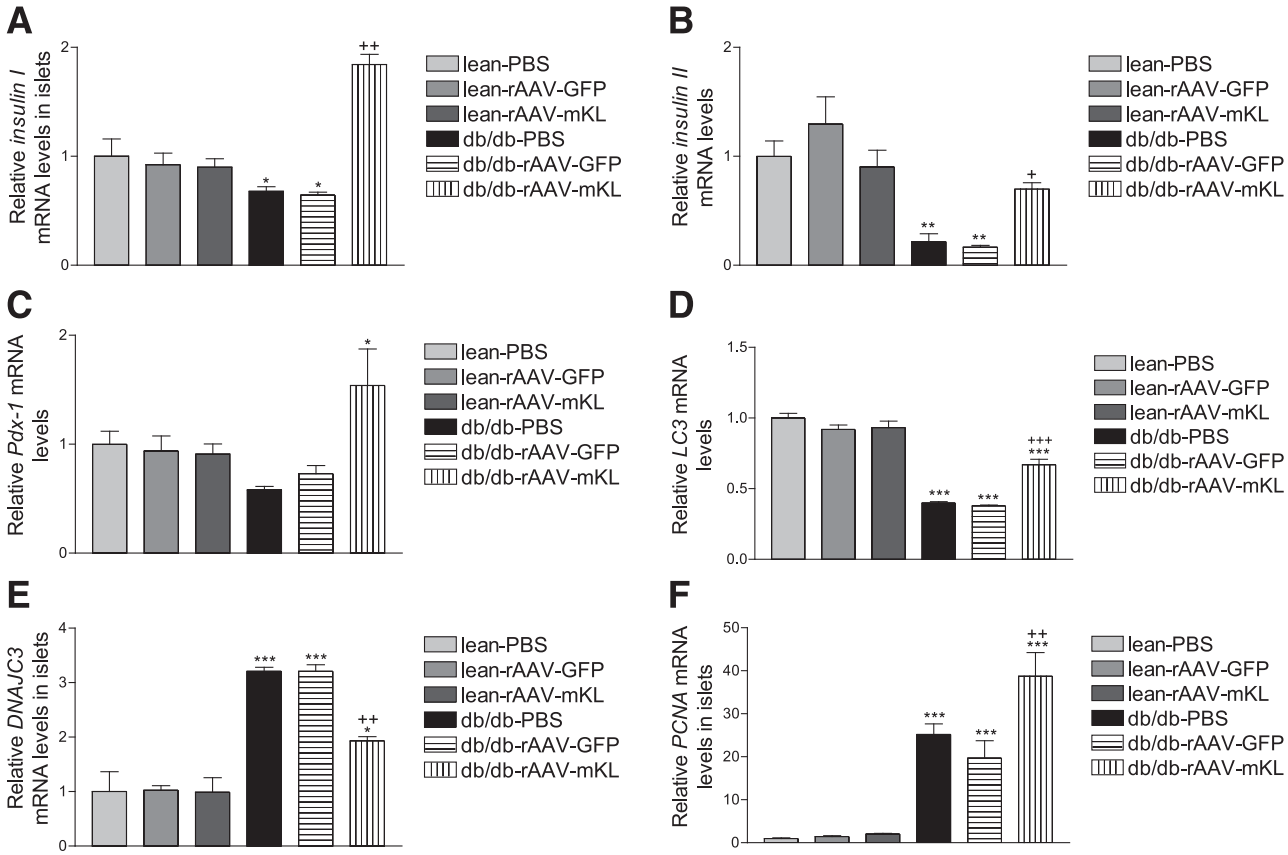


**Figure 7**—Gene expression in islets isolated from diabetic mice. Real-time RT-PCR analysis of mRNA expression of *insulin I* (*A*), *insulin II* (*B*), *Pdx-1* (*C*), *LC3* (*D*), *DNAJC3* (*E*), and *PCNA* (*F*). Results were standardized to *β-actin* mRNA levels and then expressed as fold changes vs. the lean-PBS mice. Data are mean ± SEM. $n = 3$ animals/group. *$P < 0.05$, **$P < 0.01$, ***$P < 0.001$ vs. the lean-PBS group; +$P < 0.05$, ++$P < 0.01$, +++$P < 0.001$ vs. the *db/db*-PBS group.

*Klotho* gene and protein are expressed in pancreatic islets (11). Notably, Klotho protein expression in β-cells was decreased in both patients with T2DM and *db/db* mice, a mouse model of T2DM (Fig. 1*A*–*F*). The novel finding of the current study is that β-cell–specific expression of Klotho attenuated the development of diabetes and enhanced glucose tolerance in *db/db* mice. The beneficial effects of Klotho is likely due to the increases in number of insulin-positive β-cells, insulin storage levels in pancreatic islets, and glucose-stimulated insulin secretion from pancreatic islets, which led to the increased blood insulin levels in *db/db* mice.

The depleted Klotho protein expression was associated with decreased insulin storage in pancreatic islets (Fig. 1*A*, *B*, *D*, and *E*) and the impaired glucose-stimulated insulin release in pancreatic islets of *db/db* mice (Fig. 3*F*). β-Cell–specific expression of Klotho improved or preserved β-cell function (Figs. 2 and 3). Of note, a new finding is that β-cell function may be regulated by Klotho. These findings are supported by those of our previous cell culture study that silencing of the Klotho gene impaired glucose-stimulated insulin release and that overexpression of Klotho promoted glucose-stimulated insulin secretion in MIN6 β-cells (11). Klotho enhances glucose-induced insulin secretion by regulating plasma membrane levels of TRPV2 and intracellular levels of calcium (11). Klotho-deficient mice exhibit hypoinsulinemia and pancreatic islet atrophy with diminished insulin protein and mRNA levels (10). The current study further demonstrated that β-cell–specific expression of Klotho increased *Pdx-1*, *insulin I*, and *insulin II* mRNA levels and their corresponding proteins levels in pancreatic islets of *db/db* mice. Pdx-1 is the major regulator of glucose-stimulated insulin gene transcription. Specific point mutations in *Pdx-1* are associated with maturity-onset diabetes of the young 4 and late-onset T2DM, as characterized by a decline in β-cell function (32). The present study suggests that the promoting effects of Klotho on insulin synthesis may be partially attributed to the increased Pdx-1 expression. Further study is required to elucidate the mechanism for the regulation of *Pdx-1* gene expression by Klotho in pancreatic islets.

β-Cell–specific expression of Klotho did not alter insulin sensitivity. The *insulin II* promoter was specific in driving gene expression in pancreatic β-cells because GFP was exclusively detected in pancreatic islets but was not detectable in peripheral tissues (liver and kidneys) in mice treated with rAAV-GFP (Supplementary Fig. 3*A*). rAAV-

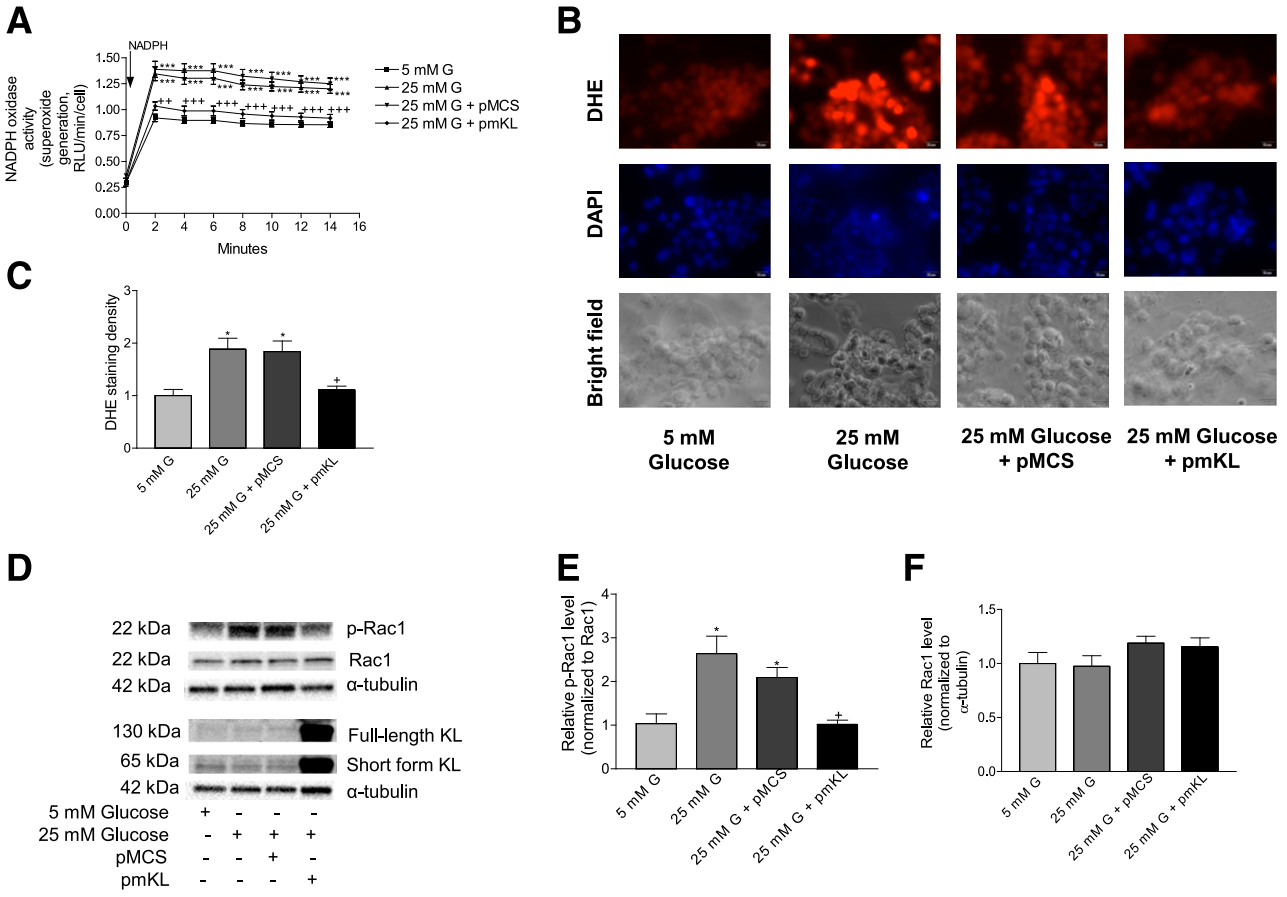


**Figure 8—**Effects of overexpression of Klotho on NADPH oxidase activity, superoxide production, p-Rac1, and Rac1 in MIN6 β-cells. MIN6 β-cells were transfected with pmKL (with FLAG-tag) or pMCS (multiple cloning site control plasmid) for 48 h and then incubated with 5 or 25 mmol/L glucose for 18 h. *A*: NADPH oxidase activity (arrow indicates addition of NADPH). NADPH oxidase activity in MIN6 cells was measured using lucigenin chemiluminescence assay. *B*: Representative images of DHE staining (superoxide production) in MIN6 β-cells. *C*: Quantification of DHE staining density. *D*: Representative Western blot bands of Klotho, p-Rac1, and Rac1 protein expressions in MIN6 β-cells. *E*: Quantification of p-Rac1. *F*: Quantification of Rac1. Results were normalized to α-tubulin level and expressed as fold changes vs. the control (5 mmol/L glucose). Data are means ± SEM. $n = 3–6$. $^{*}P < 0.05$, $^{***}P < 0.001$ vs. 5 mmol/L glucose group; $+P < 0.05$, $++P < 0.01$, $+++P < 0.001$ vs. 25 mmol/L glucose + pMCS group. G, glucose; KL, Klotho; RLU, relative light unit.

mKL was expressed in pancreatic islets as indicated by expression of FLAG-tag (Supplementary Fig. 3*C*). The *insulin II* promoter was also potent in driving *Klotho* gene expression in β-islets (Supplementary Fig. 3*D* and *E*). This promoter is as potent as the *CMV* promoter (Supplementary Fig. 1*B*).

We further explored the potential mechanisms by which β-cell–specific expression of Klotho protected against β-cell failure in pancreatic islets of *db/db* mice. rAAV-mKL decreased reactive oxygen species (ROS) and oxidative damage as measured by DHE and 4-HNE, respectively, in pancreatic islets of *db/db* mice. Oxidative stress induced by ROS is critically involved in the impairment of β-cell function during the development of diabetes (33). Because of their low antioxidant capacity, β-cells are extremely susceptible to oxidative stress (34). Hyperglycemia and hyperlipidemia cause oxidative damage to proteins, lipids, and DNA in β-cells as the result of a combination of increased free radical production and an impaired ability of cells to detoxify the radicals and repair damaged molecules (33). By covalently modifying membrane-associated proteins, the membrane lipid peroxidation product 4-HNE may play particularly sinister roles in the metabolic syndrome and associated disease processes (35).

Superoxide is the major source of ROS that causes oxidative damage, so we further explored the mechanism of Klotho-induced reduction of superoxide production under hyperglycemic conditions. Because a study of the mechanistic link of Klotho and superoxide generation may be compromised in the in vivo animal experiment, we investigated how Klotho attenuates high glucose–induced superoxide production in MIN6 β-cells. The data suggest that Klotho decreases high glucose–induced upregulation of NADPH oxidase activity and superoxide production likely through suppressing phosphorylation of Rac1 (Fig. 8), a key regulator of NADPH oxidase. Thus, this result reveals a previously unidentified role of Klotho in the regulation

of Rac1 and NADPH oxidase activity in β-cells. Of note, Klotho attenuates high glucose–induced upregulation of NADPH oxidase activity and superoxide production without alteration of glucose levels, suggesting that Klotho has a direct protective effect in β-cells. On the other hand, in the animal study, the beneficial effects of overexpression of Klotho in β-cells may also be partially attributed to the euglycemic effect of Klotho due to increased insulin secretion. Collectively, these data indicate that β-cell–specific expression of Klotho may preserve β-cells partially by suppressing superoxide production and oxidative stress in pancreatic β-islets in T2DM.

Oxidative stress could impair ER function, leading to ER stress (36,37). As a secretory cell that synthesizes and releases a large amount of insulin, the β-cell is expected to be susceptible to alterations in ER homeostasis, which can result in the accumulation of unfolded, misfolded, and/or aggregated proteins (a phenomenon known as ER stress) (38). Eukaryotic cells respond to ER stress by activating the unfolded protein response (UPR), a process that allows cells to adapt to and attempt to relieve ER stress conditions (38). Hyperactivation of the UPR is indispensible for ER homeostasis and may be involved in β-cell dysfunction and death during the progression of T2DM. The level of ER chaperone protein DNAJC3 is elevated in pancreatic islets of *db/db* mice and human T2DM (39). β-Cell–specific expression of mKL attenuated diabetes-induced increases in DNAJC3 expression in pancreatic islets (Fig. 5). Thus, this result reveals that Klotho attenuated ER stress, which may contribute to the preservation of β-cells and protection against diabetes by β-cell–specific expression of Klotho.

The current study demonstrates that β-cell–specific expression of Klotho enhances cell proliferation and decreases cell apoptosis in pancreatic islets of *db/db* mice (Fig. 6*A–D*). These results suggest for the first time that β-cell–specific expression of Klotho may preserve β-cells partially through attenuating apoptosis and promoting cell proliferation in pancreatic islets of *db/db* mice. This beneficial effect may be partially mediated by Klotho-induced suppression of superoxide production and oxidative stress, which are known to cause cell apoptosis and impair cell proliferation (40). Regulation of β-cell mass is dynamic and tightly matched to meet the body's demand for insulin (41). The rates of β-cell apoptosis or necrosis and β-cell proliferation or neogenesis equilibrate at a frequency of 0.5% under steady-state conditions (42). It was reported that β-cell apoptosis contributes to the reduction of β-cell mass in patients with T2DM (43,44). It has been shown that Klotho and FGF23 together promote cell proliferation in vitro (45,46). The current diabetic model revealed that the frequency of proliferative and apoptotic events per islet is relatively low (1–2%). We believe that the accumulated effects of proliferation and apoptosis in β-cell mass may take time.

An unexpected finding was that the expression of LC3, a marker of autophagy, decreased in pancreatic islets of *db/db* mice, whereas β-cell–specific expression of mKL reversed the downregulation of LC3 expression in islets of *db/db* mice (Figs. 5*D* and 7*D*). Autophagy is a physiologically preserved process that maintains homeostatic functions such as protein degradation and organelle turnover (47). A major member of this family is LC3, which is associated with the autophagosome from its formation to its maturation into autolysosome and serves as a bona fide marker for autophagy (48). Loss-of-function experiments ($Atg7^{f/f}$:RIP-Cre mice) have demonstrated that autophagy in β-cells is critical in the preservation of pancreatic β-cell function (49). Accumulation of p62, a substrate for autophagy, in β-cells of *db/db* mice has been observed (50). Autophagy deficiency may be involved in lipotoxicity-induced β-cell failure in T2DM (2,48). Therefore, the current study indicates that the restoration of autophagic activity by expression of Klotho may contribute to the preservation of β-cells in pancreatic islets of diabetic mice. The regulation of autophagy by Klotho may be partially attributed to suppression of superoxide production and oxidative stress, which are known to disrupt autophagy (40).

The major type of endogenous Klotho in pancreatic β-cells is ~65 kDa based on Western blot analysis (Figs. 1*C*, 1*F*, and 8*D*). Of note, overexpression of Klotho produced two types of Klotho, short form (65 kDa) and full length (130 kDa) (Fig. 8*D*, Supplementary Fig. 3*D*). However, the 65-kDa Klotho seems to be the functional protein because treatment with 65-kDa, not 130-kDa, Klotho protein promoted glucose-induced insulin secretion (Supplementary Fig. 5). Therefore, the beneficial effects of in vivo β-cell–specific expression of Klotho in T2DM may be mediated by the 65-kDa Klotho. Of note, Klotho promotes high glucose-stimulated insulin secretion in β-cells but does not affect insulin secretion at low glucose levels (Fig. 3*F*, Supplementary Fig. 5). This finding is consistent with our previous observation in MIN6 β-cells (11).

In summary, β-cell–specific expression of Klotho preserved β-cell function and protected against the development of T2DM in *db/db* mice. Particularly, β-cell–specific expression of Klotho attenuated hyperglycemia and improved glucose tolerance in diabetic mice. This protection was associated with significant increases in number of β-cells, Pdx-1 levels, and insulin storage levels in pancreatic islets; the glucose-stimulated insulin secretion from pancreatic islets; and blood insulin levels. β-Cell–specific expression of Klotho preserved β-cell function likely by suppressing oxidative stress, ER stress, and apoptosis; increasing cell proliferation; and normalizing autophagy in pancreatic islets of *db/db* mice. Therefore, in vivo expression of Klotho in pancreatic β-cells may offer a new and effective therapeutic strategy for β-cell dysfunction in T2DM. These promising findings warrant further mechanistic investigation into the role of Klotho in regulating β-cell function. β-Cell–specific expression of Klotho attenuates but does not prevent the development of T2DM; therefore, simultaneous management of hyperglycemia

and insulin resistance is also important for the protection of β-cells in T2DM.

**Funding.** This work was supported by NIH grants R01-DK-093403, HL-105302, HL-102074, and HL-118558. This publication was made possible by NIH grant 9P20-GM-104934-06 from the Centers of Biomedical Research Excellence program of the National Institute of General Medical Sciences.

**Duality of Interest.** No potential conflicts of interest relevant to this article were reported.

**Author Contributions.** Y.L. contributed to the experiments, data analysis, and writing of the manuscript. Z.S. contributed to the study concept and hypotheses, study design, and writing of the manuscript. Z.S. is the guarantor of this work and, as such, takes responsibility for the integrity of the data and the accuracy of the data analysis.

## References

1. Zimmet P, Alberti KG, Shaw J. Global and societal implications of the diabetes epidemic. Nature 2001;414:782–787
2. Leahy JL, Hirsch IB, Peterson KA, Schneider D. Targeting beta-cell function early in the course of therapy for type 2 diabetes mellitus. J Clin Endocrinol Metab 2010;95:4206–4216
3. Matthews DR, Cull CA, Stratton IM, Holman RR, Turner RC; UK Prospective Diabetes Study (UKPDS) Group. UKPDS 26: Sulphonylurea failure in non-insulin-dependent diabetic patients over six years. Diabet Med 1998;15:297–303
4. Leahy JL. Pathogenesis of type 2 diabetes mellitus. Arch Med Res 2005;36:197–209
5. Ferrannini E, Mari A. Beta cell function and its relation to insulin action in humans: a critical appraisal. Diabetologia 2004;47:943–956
6. Kuro-o M, Matsumura Y, Aizawa H, et al. Mutation of the mouse klotho gene leads to a syndrome resembling ageing. Nature 1997;390:45–51
7. Chen CD, Podvin S, Gillespie E, Leeman SE, Abraham CR. Insulin stimulates the cleavage and release of the extracellular domain of Klotho by ADAM10 and ADAM17. Proc Natl Acad Sci U S A 2007;104:19796–19801
8. Kurosu H, Yamamoto M, Clark JD, et al. Suppression of aging in mice by the hormone Klotho. Science 2005;309:1829–1833
9. Kurosu H, Kuro-O M. The Klotho gene family as a regulator of endocrine fibroblast growth factors. Mol Cell Endocrinol 2009;299:72–78
10. Utsugi T, Ohno T, Ohyama Y, et al. Decreased insulin production and increased insulin sensitivity in the klotho mutant mouse, a novel animal model for human aging. Metabolism 2000;49:1118–1123
11. Lin Y, Sun Z. Antiaging gene Klotho enhances glucose-induced insulin secretion by up-regulating plasma membrane levels of TRPV2 in MIN6 β-cells. Endocrinology 2012;153:3029–3039
12. Shafrir E. Diabetes in animals: contribution to the understanding of diabetes by study of its etiopathology in animal models. In *Diabetes Mellitus*. Porte D, Sherwin RS, Baron A, Eds. New York, McGraw-Hill, 2003, p. 231–255
13. Miyazaki J, Araki K, Yamato E, et al. Establishment of a pancreatic beta cell line that retains glucose-inducible insulin secretion: special reference to expression of glucose transporter isoforms. Endocrinology 1990;127:126–132
14. Crosswhite P, Chen K, Sun Z. AAV delivery of tumor necrosis factor-α short hairpin RNA attenuates cold-induced pulmonary hypertension and pulmonary arterial remodeling. Hypertension 2014;64:1141–1150
15. Wang X, Skelley L, Wang B, Mejia A, Sapozhnikov V, Sun Z. AAV-based RNAi silencing of NADPH oxidase gp91(phox) attenuates cold-induced cardiovascular dysfunction. Hum Gene Ther 2012;23:1016–1026
16. Wang Z, Zhu T, Rehman KK, et al. Widespread and stable pancreatic gene transfer by adeno-associated virus vectors via different routes. Diabetes 2006;55:875–884
17. Auricchio A, Hildinger M, O'Connor E, Gao GP, Wilson JM. Isolation of highly infectious and pure adeno-associated virus type 2 vectors with a single-step gravity-flow column. Hum Gene Ther 2001;12:71–76
18. Rohr UP, Wulf MA, Stahn S, Steidl U, Haas R, Kronenwett R. Fast and reliable titration of recombinant adeno-associated virus type-2 using quantitative real-time PCR. J Virol Methods 2002;106:81–88
19. Veldwijk MR, Topaly J, Laufs S, et al. Development and optimization of a real-time quantitative PCR-based method for the titration of AAV-2 vector stocks. Mol Ther 2002;6:272–278
20. Wang Y, Kuro-o M, Sun Z. Klotho gene delivery suppresses Nox2 expression and attenuates oxidative stress in rat aortic smooth muscle cells via the cAMP-PKA pathway. Aging Cell 2012;11:410–417
21. Wang Y, Sun Z. Klotho gene delivery prevents the progression of spontaneous hypertension and renal damage. Hypertension 2009;54:810–817
22. Carter JD, Dula SB, Corbin KL, Wu R, Nunemaker CS. A practical guide to rodent islet isolation and assessment. Biol Proced Online 2009;11:3–31
23. Crosswhite P, Sun Z. Ribonucleic acid interference knockdown of interleukin 6 attenuates cold-induced hypertension. Hypertension 2010;55:1484–1491
24. Wang X, Sun Z. RNAi silencing of brain klotho potentiates cold-induced elevation of blood pressure via the endothelin pathway. Physiol Genomics 2010;41:120–126
25. da Silva Xavier G, Sun G, Qian Q, Rutter GA, Leclerc I. ChREBP regulates Pdx-1 and other glucose-sensitive genes in pancreatic β-cells. Biochem Biophys Res Commun 2010;402:252–257
26. Li H, Lam A, Xu AM, Lam KS, Chung SK. High dosage of Exendin-4 increased early insulin secretion in differentiated beta cells from mouse embryonic stem cells. Acta Pharmacol Sin 2010;31:570–577
27. Lu H, Yang Y, Allister EM, Wijesekara N, Wheeler MB. The identification of potential factors associated with the development of type 2 diabetes: a quantitative proteomics approach. Mol Cell Proteomics 2008;7:1434–1451
28. Mosley AL, Ozcan S. Glucose regulates insulin gene transcription by hyperacetylation of histone h4. J Biol Chem 2003;278:19660–19666
29. Xu B, Hua J, Zhang Y, et al. Proliferating cell nuclear antigen (PCNA) regulates primordial follicle assembly by promoting apoptosis of oocytes in fetal and neonatal mouse ovaries. PLoS One 2011;6:e16046
30. Gaddy DF, Riedel MJ, Pejawar-Gaddy S, Kieffer TJ, Robbins PD. In vivo expression of HGF/NK1 and GLP-1 From dsAAV vectors enhances pancreatic β-cell proliferation and improves pathology in the *db/db* mouse model of diabetes. Diabetes 2010;59:3108–3116
31. Wang AY, Peng PD, Ehrhardt A, Storm TA, Kay MA. Comparison of adenoviral and adeno-associated viral vectors for pancreatic gene delivery in vivo. Hum Gene Ther 2004;15:405–413
32. Al-Quobaili F, Montenarh M. Pancreatic duodenal homeobox factor-1 and diabetes mellitus type 2 (review). Int J Mol Med 2008;21:399–404
33. Poitout V, Robertson RP. Glucolipotoxicity: fuel excess and beta-cell dysfunction. Endocr Rev 2008;29:351–366
34. Robertson RP. Beta-cell deterioration during diabetes: what's in the gun? Trends Endocrinol Metab 2009;20:388–393
35. Mattson MP. Roles of the lipid peroxidation product 4-hydroxynonenal in obesity, the metabolic syndrome, and associated vascular and neurodegenerative disorders. Exp Gerontol 2009;44:625–633
36. Chao YM, Lai MD, Chan JY. Redox-sensitive endoplasmic reticulum stress and autophagy at rostral ventrolateral medulla contribute to hypertension in spontaneously hypertensive rats. Hypertension 2013;61:1270–1280
37. Inoue T, Suzuki-Karasaki Y. Mitochondrial superoxide mediates mitochondrial and endoplasmic reticulum dysfunctions in TRAIL-induced apoptosis in Jurkat cells. Free Radic Biol Med 2013;61:273–284
38. Volchuk A, Ron D. The endoplasmic reticulum stress response in the pancreatic β-cell. Diabetes Obes Metab 2010;12(Suppl. 2):48–57
39. Laybutt DR, Preston AM, Akerfeldt MC, et al. Endoplasmic reticulum stress contributes to beta cell apoptosis in type 2 diabetes. Diabetologia 2007;50:752–763
40. Varga ZV, Giricz Z, Liaudet L, Haskó G, Ferdinandy P, Pacher P. Interplay of oxidative, nitrosative/nitrative stress, inflammation, cell death and autophagy in diabetic cardiomyopathy. Biochim Biophys Acta. 2 July 2014 [Epub ahead of print]

41. Finegood DT, Scaglia L, Bonner-Weir S. Dynamics of beta-cell mass in the growing rat pancreas. Estimation with a simple mathematical model. Diabetes 1995;44:249–256
42. Bonner-Weir S. Perspective: postnatal pancreatic beta cell growth. Endocrinology 2000;141:1926–1929
43. Butler AE, Janson J, Bonner-Weir S, Ritzel R, Rizza RA, Butler PC. Beta-cell deficit and increased beta-cell apoptosis in humans with type 2 diabetes. Diabetes 2003;52:102–110
44. Leonardi O, Mints G, Hussain MA. Beta-cell apoptosis in the pathogenesis of human type 2 diabetes mellitus. Eur J Endocrinol 2003;149:99–102
45. Medici D, Razzaque MS, Deluca S, et al. FGF-23-Klotho signaling stimulates proliferation and prevents vitamin D-induced apoptosis. J Cell Biol 2008;182:459–465
46. Shalhoub V, Ward SC, Sun B, et al. Fibroblast growth factor 23 (FGF23) and alpha-klotho stimulate osteoblastic MC3T3.E1 cell proliferation and inhibit mineralization. Calcif Tissue Int 2011;89:140–150
47. Levine B, Klionsky DJ. Development by self-digestion: molecular mechanisms and biological functions of autophagy. Dev Cell 2004;6:463–477
48. Las G, Shirihai OS. The role of autophagy in β-cell lipotoxicity and type 2 diabetes. Diabetes Obes Metab 2010;12(Suppl. 2):15–19
49. Ebato C, Uchida T, Arakawa M, et al. Autophagy is important in islet homeostasis and compensatory increase of beta cell mass in response to high-fat diet. Cell Metab 2008;8:325–332
50. Ichimura Y, Kominami E, Tanaka K, Komatsu M. Selective turnover of p62/A170/SQSTM1 by autophagy. Autophagy 2008;4:1063–1066